

Reciprocity Violation for Mie Scatterers at the Interface and a Scattering Solar Concentrator

Ilya Sychugov*

KTH – Royal Institute of Technology, Department of Applied Physics, 11419 Stockholm

*ilyas@kth.se

PhySH: Near-field optics, Nanoantennas, Non-reciprocal propagation

Abstract

It is shown that reciprocity of the optical path can be violated through asymmetric strength coupling via near-field from resonant Mie scatterers to total internal reflection modes in a dielectric slab. Numerical simulations for silicon nanospheres separated by a nanogap from the glass substrate reveal that at least two orders of magnitude rectification ratio can be realized for such an optical diode configuration. Implementation to a solar light harvesting device, a scattering solar concentrator, is discussed, indicating a similar efficiency is achievable as for the state-of-the-art devices based on luminescence.

Time-reversibility of Maxwell's equations for the electromagnetic field holds for systems without imaginary part of the dielectric constant [1]. That is, in the absence of heat dissipation, such as absorption or currents (Joule losses), as well as external magnetic fields along the propagation direction (Faraday effect). On the other hand, reciprocity, in a Stokes-Helmholtz sense of reversion: "if I can see you, you can see me", is related to the symmetry of the permittivity tensor. Violation of time-reversibility does not imply reciprocity breakdown; hence, the latter is more difficult to circumvent. Absorption, for example, does not violate reciprocity of the optical path, while the Faraday effect does.

Apart from fundamental interest in exploring boundaries of the reciprocity principle, facile radiation rectification is desired as a building block for a range of optical and thermal devices, with notable counterparts from electronics (diodes, isolators, etc.) [2,3]. Typically, variations of the Faraday effect or optical non-linearities, such as Kerr effect, including time-modulation, are used for this purpose [4]. Recently it was demonstrated that dielectric nanostructures with Mie resonances generate strong radiative nano-antenna effects and, combined with low absorption, are promising towards new nanophotonic functionalities [5].

In this paper a method for reciprocity violation is proposed, which is based on near-field coupling to and from the resonant Mie scatterer at the interface. A total internal reflection (TIR) mode in a planar dielectric substrate (glass) is considered with a spherical Mie particle (silicon) placed above it. It is shown that the excitation of the TIR mode takes place efficiently across the near-field gap for the resonant scattering. The reciprocal process, on the other hand, is strongly suppressed due to the evanescent wave nature of the TIR mode in the nanogap. Numerical solutions to the Helmholtz equation for monochromatic waves in 3D were found for a set of geometries and wavelengths to quantify this effect. Results reveal that Si nanospheres with resonant scattering in the 400-1000 nm range can realize optical rectification ratio of at least two orders of magnitude. A particular application for solar light harvesting, namely a scattering solar concentrator, is proposed based on this effect.

First, the underlying mechanism is qualitatively illustrated in Fig. 1. A propagating TIR mode in a dielectric slab polarizes elementary bound dipoles in the opposite way at the interface. Thus, their contributions are largely canceled out outside the slab, leading to the well-known evanescent near-field [6]. Its intensity is exponentially decaying from the glass/air interface with a decay length constant $x_{1/e} = \lambda / 4\pi\sqrt{n^2 \cdot \sin^2\theta - 1}$, where n is the glass refractive index, θ is the incident TIR angle from normal, and λ is the free-space wavelength. This is valid for all angles above the critical angle, i.e. $\theta > 42^\circ$ for glass-air interface, where TIR takes place. Numerically, for $\lambda = 600$ nm and $\theta = 50^\circ, 60^\circ, 70^\circ$ the values are $x_{1/e} = 84, 57, 48$ nm. On the other hand, for resonant Mie scattering from a Si nanoparticle (NP) the material dipoles are well aligned, resulting in an efficient coupling of radiation to the scattering mode [7]. Here, the near-field is weakly decaying in the scattering direction, on the order of r^{-1} . Quantitatively, it stretches out ~ 200 nm from the 87 nm radius Si NP in air, as analytical Mie theory directly shows (Fig. S1). Note that out-of-resonance field is weaker and decays much stronger, on the order of r^{-3} (Fig. S1). Ordinary spherical particles without a resonance, such as made of glass, are known to have their near-field vanishing exponentially with a decay length on the order of the NP radius [6].

Thus, under the same excitation the near-field intensity will differ markedly for resonant Mie scatterers and planar waveguides, stemming from different elementary dipole orientations. When these two are brought together over a nanogap, one might expect even stronger coupling from the NP to the glass substrate due to a higher density of optical modes in it [8]. However, Mie theory is not applicable for such realistic inhomogeneous optical environments, requiring extensive numerical calculations to accurately quantify this interplay.

Here, a 3D model for a Si NP on glass has been built and solved with a finite element method in frequency domain for the incoming field from the substrate direction (Fig. S2). For a given wavelength, first, the background field was computed in the absence of a nanoparticle to arrive at purely nanoparticle-induced scattering fields. After solving the electromagnetic wave equation for the electric field, a normal component of the Poynting vector was integrated over chosen far-field surfaces. When normalized to the incident intensity it yields probabilities of different processes: backscattering to the substrate (σ_{BS} , lower half space), forward scattering to the air (σ_{FS} , upper half space), absorption (σ_{ABS} , inside the NP), backscattering to the escape cone (σ_{EC} , a cone with a half angle equal to the critical angle of 42^0 in the substrate), and to the waveguiding total internal reflection mode ($\sigma_{TIR} = \sigma_{BS} - \sigma_{EC}$, to the substrate outside of the escape cone). To extend the defined limited geometrical volume to infinity a Floquet boundary condition was applied. To obtain response for non-polarized light two orthogonal incoming light polarizations were calculated and the average value is reported. Glass was considered absorption-free with refractive index of 1.5, while real and imaginary parts of the refractive index for Si were taken from [9] for the spectral range considered. Calculations were performed as a function of the incidence angle, wavelength, NP size, and its distance from the substrate (nanogap). The model was first validated by comparing it with Mie theory when the substrate is replaced with air, resulting in a very good match (Fig. S3).

In Fig. 2 resulting spectra for the defined above probabilities are shown for a 87 nm radius Si NP on glass for normally incident unpolarized light. It is seen that for resonant wavelengths (550-670 nm) backscattering to the substrate dominates. For larger (smaller) particles the spectral response is similar, but the resonance range is shifted to longer (shorter) wavelengths (Fig. S4). Larger (smaller) particles have expectedly larger (smaller) absolute values of the respective cross-sections (Fig. S4).

Using this model, the process of coupling from the TIR mode to the NP as a function of the nanogap can be described quantitatively. The total interaction probability ($\sigma_{BS} + \sigma_{FS} + \sigma_{ABS}$) is shown in Fig. 3, top. For reference, the total cross-section under normal incidence is also provided (blue), which is nearly constant, as expected. It turns out that for TIR modes the interaction strength over the nanogap decays exponentially with decay constants 81, 54, and 45 nm for 50^0 , 60^0 , and 70^0 (unpolarized light). These values are obtained by integrating over the whole 400-1000 nm spectrum. Taking into account that the first moment of the total interaction cross-section distribution is ~ 600 nm for the 87 nm radius Si NP (cf. Fig. 2), there is a very good match with the analytical predictions for the evanescent wave given above.

To facilitate description in the presence of angular distribution for the TIR mode, values at 60^0 will be used as an average characteristic angle in a first approximation (the total range is from 42^0 to 90^0). Larger (smaller) particles appear to have longer (shorter) decay constants for this

incidence TIR angle (Fig. S5). These values almost linearly scale with the average interaction wavelength (cf. Fig. S4) and, again, coincide well with the analytical prediction for the evanescent wave intensity decay over a nanogap. Provided calculations for different size NPs and angles confirm that the coupling from the TIR mode to the NP still takes place through the evanescent wave. This is the first result of the presented analysis, revealing that a dielectric subwavelength NP does not substantially modify the TIR mode in this geometry.

Next, a reciprocal process of coupling from a NP to TIR modes is considered. First, when comparing interaction probabilities with corresponding values for a NP in air, it becomes clear that the substrate does affect spatial distribution of the scattered light (Fig. S6). A higher density of optical modes indeed enhances BS probability (from 34% to 46% over the whole spectrum for a 87 nm radius particle) for normal incidence. As a result, a large fraction of the incoming light is coupled to the slab TIR mode ($\sim 27\%$ for all sizes considered; the absolute values are larger for bigger particles, cf. Fig. S4). For incoming angles other than normal this result holds, except for the critical angle, where peculiar polarization-related effects are observed [10].

So, the difference qualitatively depicted in Fig. 1 is, in fact, enhanced when a NP is brought to the near-field substrate proximity. Now we can explicitly compare the strength of in- and outcoupling of light to/from the TIR mode over a nanogap (full spectra are shown in Fig. S7). In Fig. 3, bottom, the probability of coupling to the TIR mode is presented (blue) for three different NP sizes as a function of the spacing (for normal unpolarized incidence). The interaction strength decays slowly and can be fitted well with a single exponential function with decay constants 4.5-5 times longer than that of the TIR-NP total cross-section (cf. Fig. 3, top and Fig. S6). As far as optical path reversibility is concerned, the coupling of normal incident light to the TIR mode is reciprocal to the coupling from the TIR mode to the escape cone. Specific cross-section for the latter is shown in Fig. 3, bottom, as a black line. It is seen that this probability drops very quickly, essentially being limited by the evanescent wave as indicated by the decay constant value of ~ 50 nm.

Altogether, already at the nanogap value of ~ 170 nm a two orders of magnitude rectification ratio can be achieved (red arrow in Fig. 3, bottom). Thus, this configuration is similar to the asymmetric tunneling junction in electronics, facilitating a one-way traffic for the electromagnetic wave. For reasons explained below, spectrally integrated values for unpolarized light were mainly considered here. Should the rectification ratio be the main parameter of interest, it can potentially be enhanced even further by using specific wavelengths with a given polarization in conjunction with the shape-controlled nanoparticles, such as nanorods. Collective effects in Mie resonators [11], which can be fabricated from other materials as well [12], can also be invoked to optimize this diode-like effect.

Practically, large amounts of Si nanospheres can at present be fabricated by different methods with a narrow size dispersion [13,14]. Solutions of these nanoparticles can be spray-coated or self-assembled on the surface using, e.g., Langmuir-Blodgett method. Hollow polymer nanospheres may serve as a nearly optically passive nanogap, supporting Si nanoparticles [15]. Alternatively, for the spacer formation, NP resonators can be placed on aerogels or highly porous polymer films with refractive index close to unity of a desired thickness [16].

Presented here light coupling to and from the TIR mode is usually not considered in far- or near-field microscopy, where illumination/collection takes place in the far-field transmission [17,18]. For some applications, however, it is exactly the TIR mode excitation and its outcoupling, which define the device performance. One such application is illustrated here in detail, namely a scattering solar concentrator (SSC).

It is analogous with a luminescent solar concentrator (LSC), where solar radiation is converted to luminescence for subsequent TIR waveguiding and collection at the slab edges by standard solar cells [19]. Here typical fluorophores possess good absorption in the visible range and low absorption at the emission wavelengths in the near-infrared (Stokes shift) to suppress re-absorption. Thus, time-reversibility is broken by carrier thermalization (down-conversion), which allows light to be coupled to the TIR mode ($\sim 75\%$ for embedded isotropic emitters in a glass/polymer), at the same time suppressing the reverse process. Attempts to realize such a device based on scattering were not successful due to the optical path reversibility: the in-coupled light can be easily out-coupled, detrimental to waveguiding for large area slabs [20].

Using the reciprocity violation introduced here an efficient SSC device becomes possible. In SSCs a broad solar spectrum can be utilized, as opposite to a limited range in LSCs, by, e.g., combining different size Si NPs. A specific example is shown in Fig. 4. Here the TIR mode coupling probability σ_{TIR} (green, for normal incidence) is calculated for a combination of NPs (radius 66.5/87/110 nm with a relative surface density 2:1:1) located on a 150 nm nanogap from the glass substrate. The corresponding waveguiding losses are shown in black, which is $\sigma_{EC} + \sigma_{FS} + \sigma_{ABS}$ for 60° TIR incidence. The difference between them in the given spectral range is 5-10 times. In SSCs losses take place when the TIR mode encounters the surface. Then, the waveguiding efficiency can be estimated as $\eta_{wvgd} \approx [1 - (\sigma_{EC} + \sigma_{FS} + \sigma_{ABS}) \cdot n]^{0.14\delta}$, where δ is the aspect ratio of a square slab with side length a and thickness Δ : $\delta = a/\Delta$, and n is NP surface density (see Supplementary S1 for derivation). For a few NP per μm^2 surface density 6-7% of the solar power can be coupled to the TIR mode in this case. Then, for a 30x30 cm^2 device with 0.7 cm thickness, matching a Si-based solar cell width covering the edge, the waveguiding efficiency is $\sim 90\%$. Thus, optical efficiency of 5-6 % can be achieved, which is comparable in performance with similar size state-of-the-art LSCs [21,22].

Such devices are considered today as possible energy-generating glazing building envelopes and their visible light transmittance and colors are also important characteristics. For SSCs these can be tuned by selecting size and surface density of NPs with resonances in the visible range separately from the ones in the NIR range, which can be optimized solely for power generation. Other concepts for light trapping and propagation across interfaces, which heavily rely on the optical path reciprocity [23], can be also reconsidered and modified using suggested approach, resulting in new and unexpected functionalities.

To summarize, a method for reciprocity violation was suggested and numerically quantified for Si Mie resonators placed over a nanogap from the dielectric substrate. A rectification ratio of at least two orders of magnitude is predicted for light coupling to and from the total internal reflection modes. An unoptimized solar harvesting device based on this principle appears to feature at least similar performance as conventional luminescence solar concentrators.

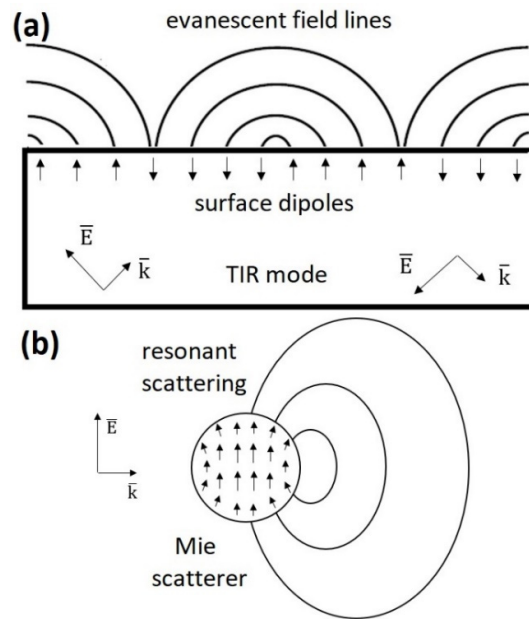


Fig. 1 Schematic representation of a difference between (a) evanescent field from a TIR mode with surface dipoles cancelling out each other, and (b) resonant “electric dipole” scattering from a Mie nanoparticle. Near-field is reaching out substantially further in (b) due to elementary dipole alignment.

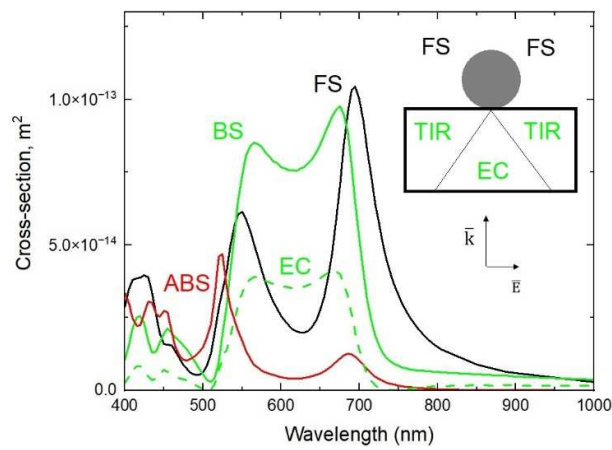


Fig. 2 Example of obtained spectral probabilities for different processes (forward scattering to the air, FS; backscattering to the substrate, BS; backscattering to the escape cone, EC; absorption in the nanoparticle, ABS) for a 87 nm radius Si NP on glass under normal incidence and (inset) schematics of the geometry used for calculations.

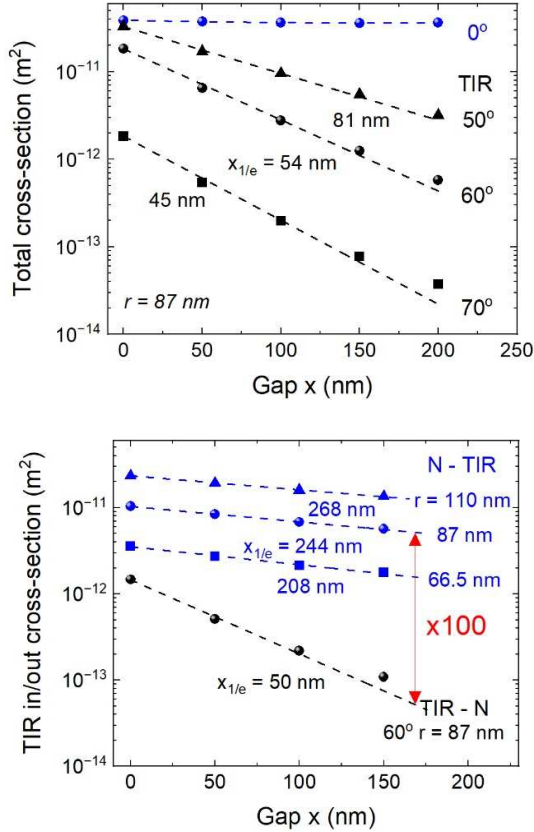


Fig. 3 (top) Total interaction probability for the incoming light at different angles from normal as a function of the nanogap for a 87 nm radius Si NP. Unpolarized light was considered (averaged over two orthogonal polarizations). TIR modes are shown in black. (bottom) Coupling probabilities to the TIR mode for different size NPs for normal incidence (blue), and the coupling probability for the TIR 60° incidence to the escape cone for a 87 nm NP (black). At the 170 nm nanogap two orders of magnitude rectification can be achieved.

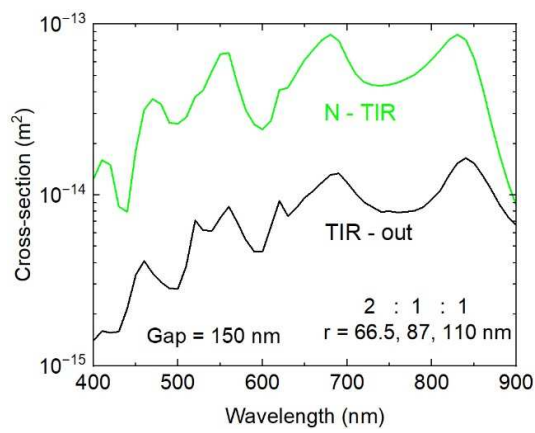


Fig. 4 Spectral response of a proposed scattering solar concentrator device. Useful scattering probability to the TIR mode (green) and total losses (black) for a combination of NPs of different sizes placed over a nanogap of 150 nm on a glass substrate.

References

- [1] O. Sigwarth and C. Miniatura, AAPPS Bulletin **32**, 23 (2022).
- [2] Z. N. Zhang and L. X. Zhu, Phys. Rev. Appl. **18**, 027001 (2022).
- [3] C. Caloz, A. Alu, S. Tretyakov, D. Sounas, K. Achouri, and Z. L. Deck-Leger, Phys. Rev. Appl. **10**, 047001 (2018).
- [4] D. L. Sounas and A. Alu, Nat. Photonics **11**, 774 (2017).
- [5] A. I. Kuznetsov, A. E. Miroshnichenko, M. L. Brongersma, Y. S. Kivshar, and B. Luk'yanchuk, Science **354**, aag2472 (2016).
- [6] M. Ohtsu and K. Kobayashi, *Optical Near Fields* (Springer-Verlag, Berlin, 2004), Introduction to Classical and Quantum Theories of Electromagnetic Phenomena at the Nanoscale, p. 17.
- [7] A. E. Miroshnichenko, A. B. Evlyukhin, Y. F. Yu, R. M. Bakker, A. Chipouline, A. I. Kuznetsov, B. Luk'yanchuk, B. N. Chichkov, and Y. S. Kivshar, Nat. Commun. **6**, 8069 (2015).
- [8] I. Sychugov, H. Omi, and Y. Kobayashi, Opt. Lett. **33**, 1807 (2008).
- [9] D. E. Aspnes and A. A. Studna, Phys. Rev. B **27**, 985 (1983).
- [10] J. Xiang, J. Li, Z. Zhou, S. Jiang, J. Chen, Q. Dai, S. Tie, S. Lan, and X. Wang, Laser Photon. Rev. **12**, 1800032 (2018).
- [11] H. Negoro, H. Sugimoto, T. Hinamoto, and M. Fujii, Adv. Opt. Mater. **10**, 2102750 (2022).
- [12] F. Vennberg, A. P. Ravishankar, and S. Anand, Nanophotonics **11**, 4755 (2022).
- [13] H. Sugimoto, T. Okazaki, and M. Fujii, Adv. Opt. Mater. **8**, 2000033 (2020).
- [14] M. A. Eslamisaray, P. R. Wray, Y. Lee, G. M. Nelson, O. Ilic, H. A. Atwater, and U. R. Kortshagen, Nano Lett. **23**, 1930 (2023).
- [15] S. H. Im, U. Y. Jeong, and Y. N. Xia, Nat. Mater. **4**, 671 (2005).
- [16] H. Budunoglu, A. Yildirim, M. O. Guler, and M. Bayindir, ACS Appl. Mater. Interfaces **3**, 539 (2011).
- [17] K. Imura and H. Okamoto, Opt. Lett. **31**, 1474 (2006).
- [18] M. Adachi, H. Sugimoto, Y. Nishimura, K. Morita, C. Ogino, and M. Fujii, Small **19**, 2207318 (2023).
- [19] W. H. Weber and J. Lambe, Appl. Opt. **15**, 2299 (1976).
- [20] Y. Li, Y. Sun, and Y. Zhang, Solar Energy **198**, 151 (2020).
- [21] J. Huang, J. Zhou, E. Jungstedt, A. Samanta, J. Linnros, L. Berglund, and I. Sychugov, ACS Photonics **9**, 2499 (2022).
- [22] N. S. Makarov, D. Korus, D. Freppon, K. Ramasamy, D. W. Houck, A. Velarde, A. Parameswar, M. R. Bergren, and H. McDaniel, ACS Appl. Mater. Interfaces **14**, 29679 (2022).
- [23] M. Majic, W. R. C. Somerville, and E. C. Le Ru, Phys. Rev. A **103**, L031502 (2021).

Reciprocity Violation for Mie Scatterers at the Interface and a Scattering Solar Concentrator

SUPPLEMENTARY MATERIAL

Ilya Sychugov

KTH – Royal Institute of Technology, Department of Applied Physics, 11419 Stockholm

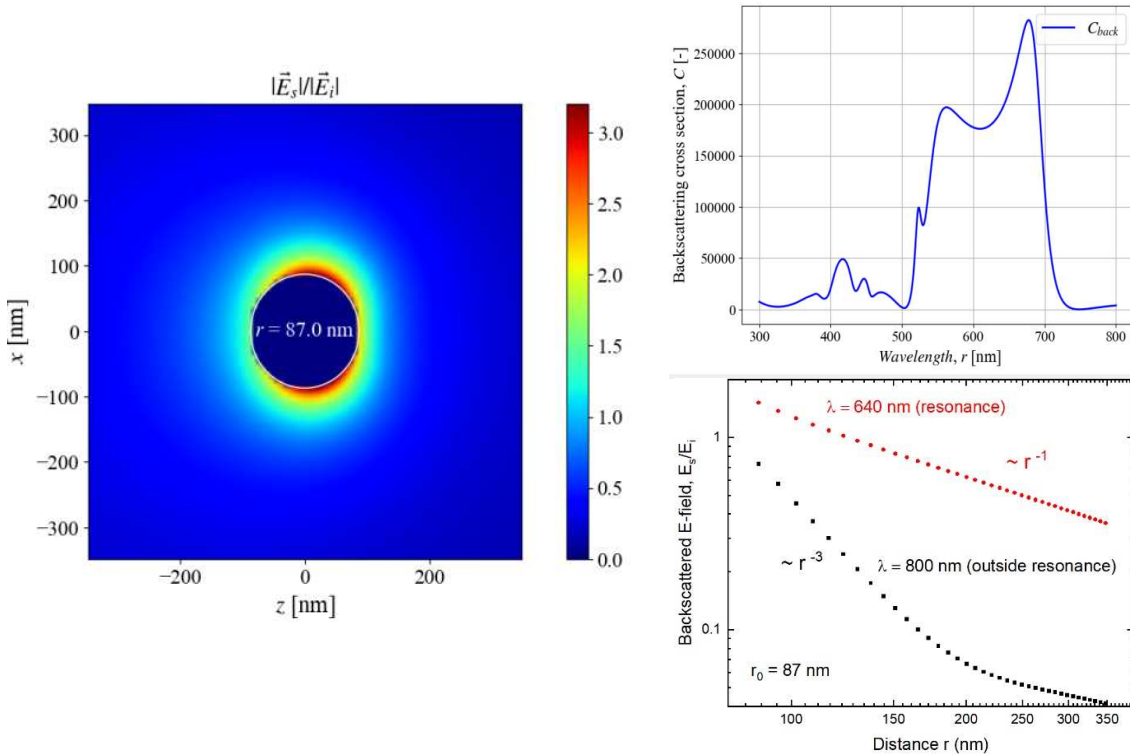


Fig. S1. (left) Scattering electric field distribution from a Si nanosphere in air with 87 nm radius under 640 nm excitation incoming from left (from PyMieLab software). This wavelength corresponds to backscattering resonance, as seen from the backscattering (“-z” direction) cross-section wavelength dependence (right, top). The near-field decays weakly for the resonant wavelength, as the scattering field profile taken at $x=0$ and $z<-87$ nm along “-z” direction shows (right, bottom).

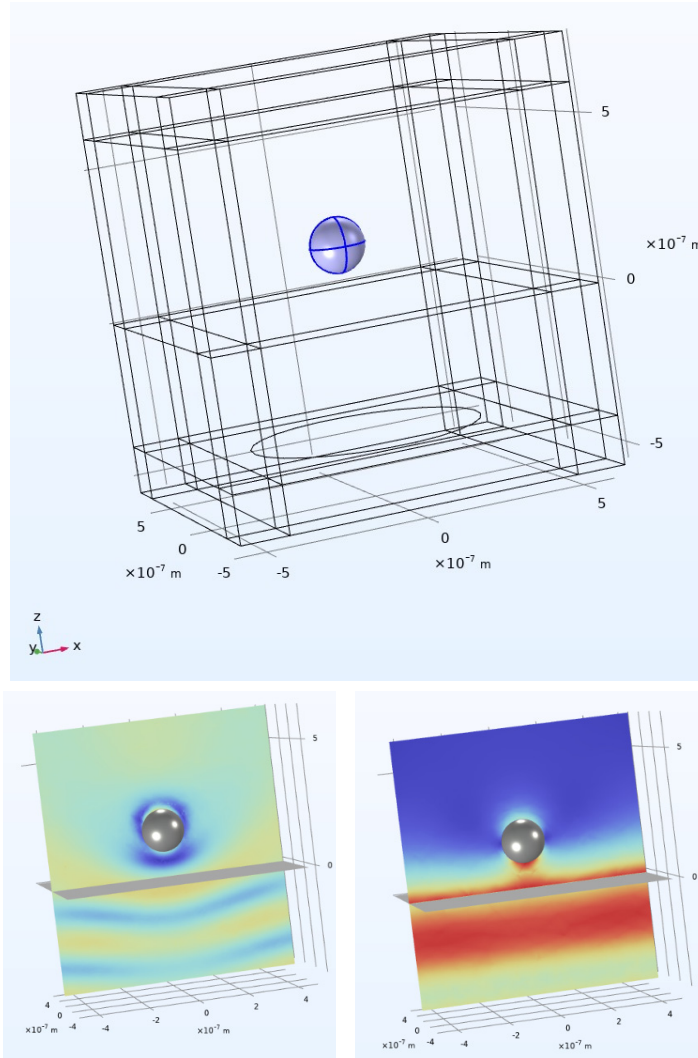


Fig. S2 (top) 3D finite-element Comsol model for a Si NP (blue) on glass (below). The circle in the bottom plane is the escape cone. Absorbing layer of $\lambda/4$ thickness surrounds the calculation volume: height in the air is λ , in the glass is $\lambda/1.5$, the width is $3\lambda/2$ (using a larger volume cube was found to modify results only by a few percent). Two orthogonal polarizations were considered: $\bar{E}_1 = (0; 1; 0)$ and $\bar{E}_2 = (\cos\theta; 0; -\sin\theta)$ for the incident angle θ from normal. (bottom) Calculated electric field distribution for 87 nm radius Si NP and 640 nm wavelength (left) for normal incidence and (right) for 60° TIR incidence.

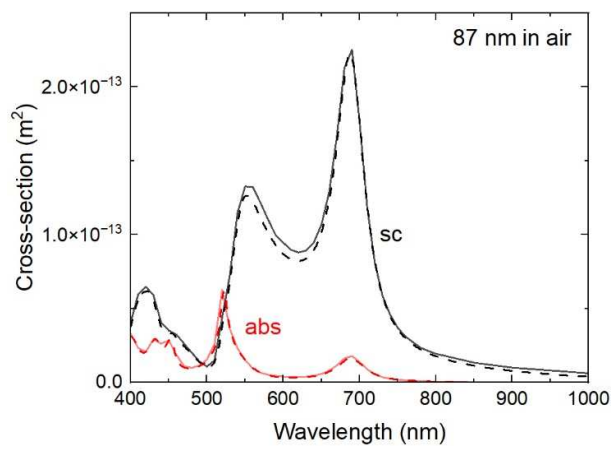


Fig. S3 Comparison of the Mie theory (dotted lines, from PyMieLab software) with the present numerical model for a Si NP with 87 nm radius in air. Total scattering (black) and absorption (red) cross-sections shown.

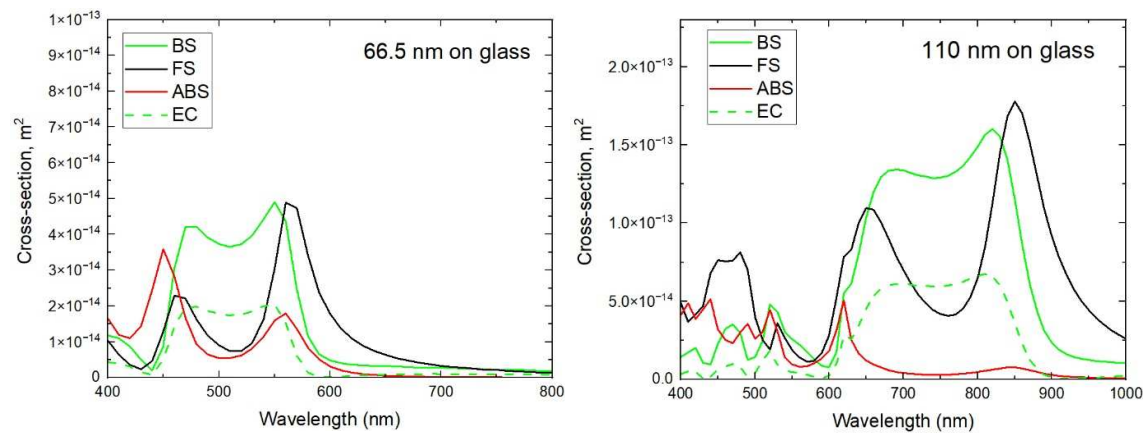


Fig. S4 Interaction probabilities for different size Si NP on glass for normal unpolarized incidence from the substrate (left) 66.5 nm radius, (right) 110 nm radius.

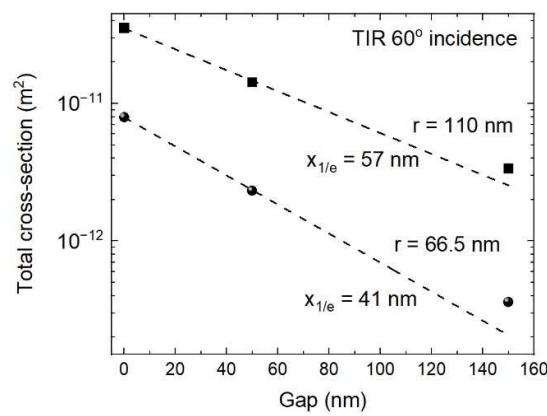


Fig. S5 Total cross-section for 60° incident TIR mode for 66.5 nm and 110 nm radius Si NPs. Decay constants scale with the average interaction wavelength.

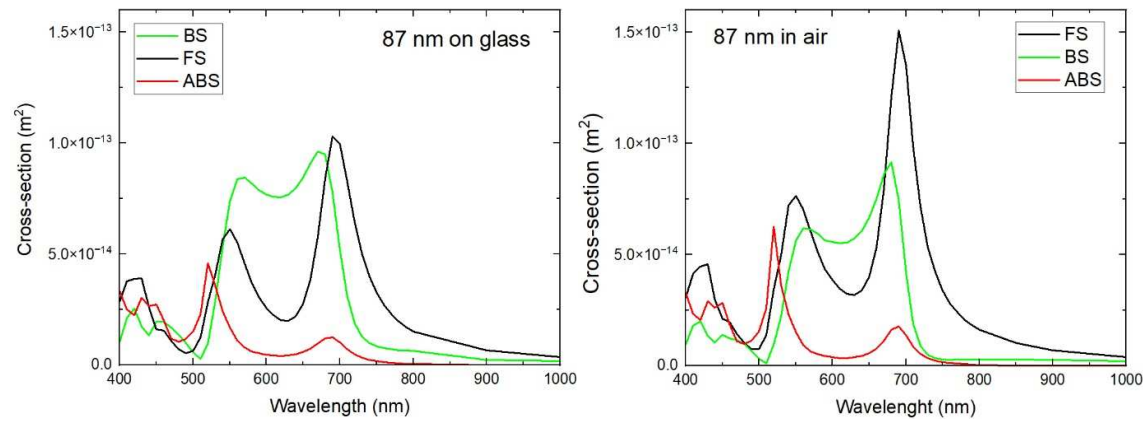


Fig. S6 Comparison of the interaction probabilities for the same size Si NP (left) on glass and (right) in air under unpolarized normal incidence. Stronger backscattering (BS, both absolute and relative) in the presence of a substrate is clear.

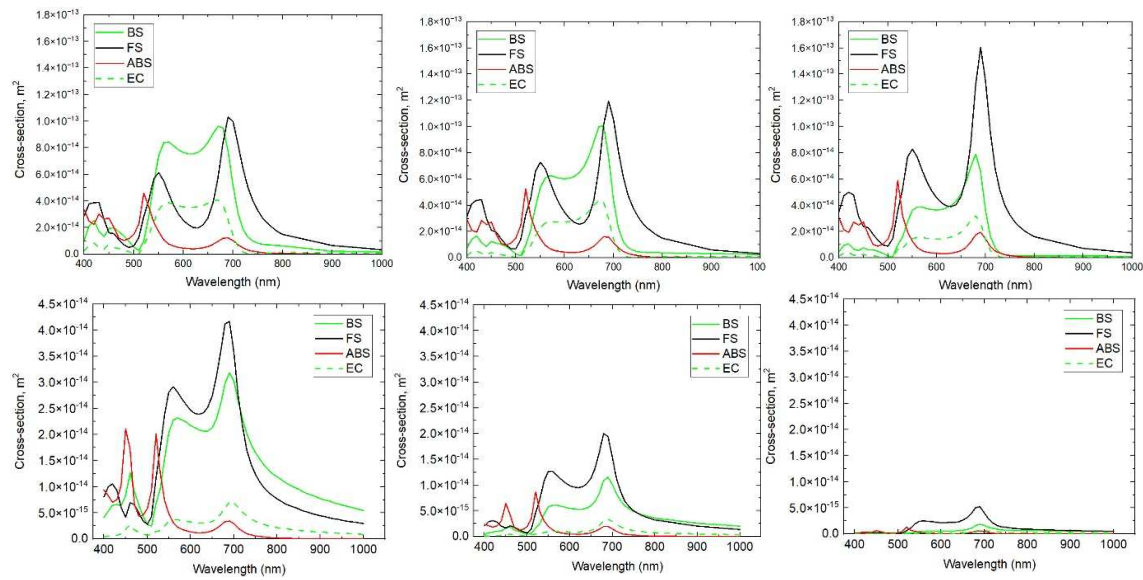


Fig. S7 Spectral distributions for the 87 nm radius Si NP (top) under normal incidence, and (bottom) for 60° TIR incidence. From left to right: NP on the surface, 50 nm gap, 150 nm gap.

S1. Waveguiding efficiency of a Scattering Solar Concentrator.

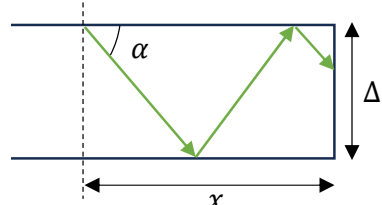
Consider a square dielectric slab (glass or polymer) with thickness Δ and side length a , $\Delta \ll a$. For the top slab surface with uniformly distributed scattering NPs we are first looking for how many times, on average, the TIR mode will encounter this layer before reaching the edge.

Let the incoming TIR mode position is at a distance x from the edge and it enters the substrate at an angle α from the horizontal plane. The valid range for α is from 0° to 48° (critical angle is 42° for the glass/air interface).

For simplicity the average value of $\alpha = 30^\circ$ can be taken.

Then the average number of encounters with the top layer for TIR mode:

$$N = \frac{x}{2\sqrt{3}\Delta}$$



The average optical path to the edge for a 2D square with uniformly distributed sources is $\sim 0.473a$ (*Appl. Opt.* 59, 5715, 2020). For the slab aspect ratio $\delta = a/\Delta$ the result becomes:

$$N \approx 0.136 \cdot \delta$$

The probability to escape TIR mode when encountering the surface layer is $(\sigma_{EC} + \sigma_{FS} + \sigma_{ABS}) \cdot n$, where n is the surface density of NPs. Thus, for N encounters the probability to reach the edge (waveguiding efficiency) is:

$$\eta_{wvgd} = [1 - (\sigma_{EC} + \sigma_{FS} + \sigma_{ABS}) \cdot n]^N$$